The 2013 World Congress on
Advances in Structural Engineering and Mechanics (ASEM13)
Jeju, Korea, September 8-12, 2013

An experimental study on cyclic behaviour of extended end-plate connections equipped with shape memory alloy bolts

*Cheng Fang[1)], Michael C.H. Yam[2)],
Angus C.C. Lam[3)] and Chuanglong Jiang[4)]

[1)] *Department of Civil & Environmental Engineering, Imperial College London, SW7 2AZ, United Kingdom, Formerly: Department of Building & Real Estate, The Hong Kong Polytechnic University, Hung Hom, Kowloon, Hong Kong SAR, China*
[2)] *Department of Building & Real Estate, The Hong Kong Polytechnic University, Hung Hom, Kowloon, Hong Kong SAR, China*
[3),4)]*Department of Civil & Environmental Engineering, University of Macau, Macau SAR, China*
[1)] c.fang@imperial.ac.uk

ABSTRACT

In parallel with the research efforts for clearer insights into the response of conventional structures against seismic effects, recent research interests have been directed to innovative construction materials to be employed as alternative solutions. The ability of shape memory alloys (SMAs) to undergo reversible deformations up to around 8% strain with moderate energy dissipation capacities makes them nowadays under active studies for seismic design purposes. This paper explores the feasibility of SMA bolts used for extended end-plate connections through experimental studies. The basic idea is to concentrate the earthquake induced deformation into the connection, such that a 'super-elastic' hinge can be formed via the elongation of the SMA bolts. The connecting column and beam including the end-plate are expected to behave elastically. Two tests, considering two different SMA bolt lengths, were conducted. The connections were tested under static cyclic loading until the occurrence of fracture in the SMA bolts. It was mainly observed that the connection with the SMA bolts had a very good recentring ability with moderate energy dissipation. Ductility of the connections was less satisfactory due to the relatively early fracture of the furthest bolt in the threaded area. The early fracture of bolts might be avoided in future through increasing the net threaded area. In addition, slight degradation of rotational stiffness was observed as the cycle number increased.

1. INTRODUCTION

The 1994 Northridge and 1995 Kobe earthquakes exposed deficiencies of welded steel connections which were expected to provide full restraints against seismic action

[1)] Post-doctoral Research Associate
[2)] Associate Professor
[3)] Assistant Professor
[4)] Research Student

(FEMA 2000). During the two major earthquakes, weld fractures observed in a large number of such connections raised the concern of their ductility, and investigations to seek alternative solutions were boosted since then. Several strengthening strategies on welded connections were proposed, and it was also recommended that the beam section near a connection could be weakened to prevent failure in the connection (Jones *et al*. 2002). It was later found that if appropriately designed, bolted connections could also offer good seismic performance due to their sound ductility and rigidity (FEMA 2000). The above design and retrofitting strategies share a common working principle: to force the formation of the plastic hinge in the beam away from the connection. While a structural system employing the above connection design strategies could have sound ductility and strength to resist seismic loading, the unrecoverable post-earthquake deformation of the beam, e.g. local buckling of the flanges, can be costly and difficult to repair.

To address this issue, a proof-of-concept connection utilizing a unique class of metal, namely, NiTi Shape Memory Alloy (SMA), is examined in this paper. SMAs have received great attention recently due to their ability to undergo reversible deformations either by heating (shape memory effect) or through unloading (superelastic effect), depending on their thermal-mechanical states. More detailed information on NiTi SMA can be found in Lagoudas (2008). A few research outcomes have already shown the effectiveness of various structural elements employing SMA components, e.g. passive seismic isolators (Dolce *et al*. 2001, Wilde *et al*. 2000), building bracings (McCormick *et al*. 2007a, Yang *et al*. 2010), and steel beam-to-column connections (Ocel *et al*. 2004, Speicher *et al*. 2011).

The basic principle of the innovative connection examined in this study is to replace the conventional high strength (HS) bolts in extended end-plate connections with superelastic SMA bolts, such that ‘superelastic hinges’ can be formed in these connections which are endowed with both self-centring and energy dissipation capabilities due to the unique characteristic of the SMA. Unlike the conventional earthquake resisting connections, the main deformation of the SMA connection is expected to concentrate in the SMA bolts, while the remaining parts, including the beam, column, and end-plate, are mainly in the elastic range. This idea was firstly proposed by Ma *et al*. (2007), and a numerical study was performed which showed that this concept was feasible. To further provide test evidence on such connections, two tests were performed by the authors. The hysteretic moment-rotation curves of the connections are presented, and the recentring ability, energy dissipation ability, rigidity, and ductility properties are examined and discussed in detail. Some critical lessons drawn from this study are also discussed.

2. TEST PROGRAMME

Stiffened extended end-plated connections with four rows of bolts were considered as the typical connection type in this study. Two connection specimens were tested, where the geometric details are illustrated in Fig. 1. Utilizing the superelastic properties of the SMA bolts, self-recentring of the connection can be enabled. The column with 1.7 m in height was fixed to a supporting frame via two rigid connections at the two column

ends, and the column was deliberately designed using an overly large size section (with negligible deformation caused during the loading process) for repeatable use. The 1.6 m length cantilever steel beam was connected to the column via eight SMA bolts through an end-plate with a thickness of 28 mm. Beam flange stiffeners were applied to reinforce the beam which was designed to behave elastically during the test. Since the main deformation is concentrated within the bolts, sufficient bolt length is desirable to achieve a reasonable ductility supply. Therefore, thick bolt washers were employed. The test code was designated according to the diameter and length of the SMA bolt used; therefore, SMA-D16-240 represents the specimen with 16 mm shank diameter and 240 mm long (including the threaded part) SMA bolts, and SMA-D16-290 represents the specimen with 16 mm shank diameter and 290 mm long SMA bolts. The shank area of the SMA bolt was similar to the net threaded area. A preload of approximately 70% of the yield strength (forward transformation stress) was applied to each SMA bolt.

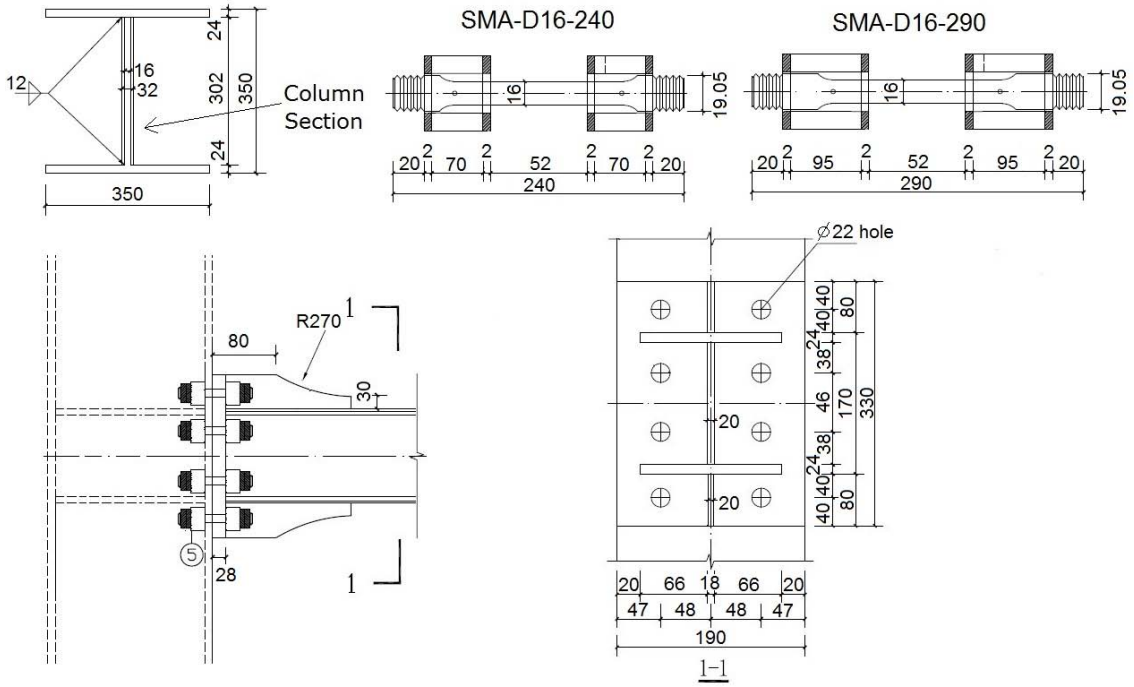

Fig. 1 Geometric properties for test specimens

The raw SMA bars, which were later machined to the SMA bolts, were ordered from the supplier SAES Smart Materials (www.memry.com). All bars have sufficiently low austenite start temperatures (around -10ºC) to allow superelastic behaviour at ambient temperatures. The composition of all the SMA bars was almost identical, with nickel by weight ranging from 55.86% to 55.94% and the remaining weight was contributed by titanium. The bars were hot-rolled, and were heat treated with an annealing temperature of 454°C/850°F (kept for 30 minutes), and then air cooled. The heat

treatment was conducted by the commercial supplier, and no further heat treatment was performed on the as-received bars. The mechanical properties of the as-received bars were tested by applying cyclic tensile loading on dog bone tensile specimens, and the typical stress-strain curves are shown in Fig. 2. The average modulus of elasticity and the yield strength (forward transform stress) of the SMA tensile bars were 40 GPa and 350 MPa, respectively. For the column, S355 steel was employed, and S275 steel was employed for all end-plates and beams.

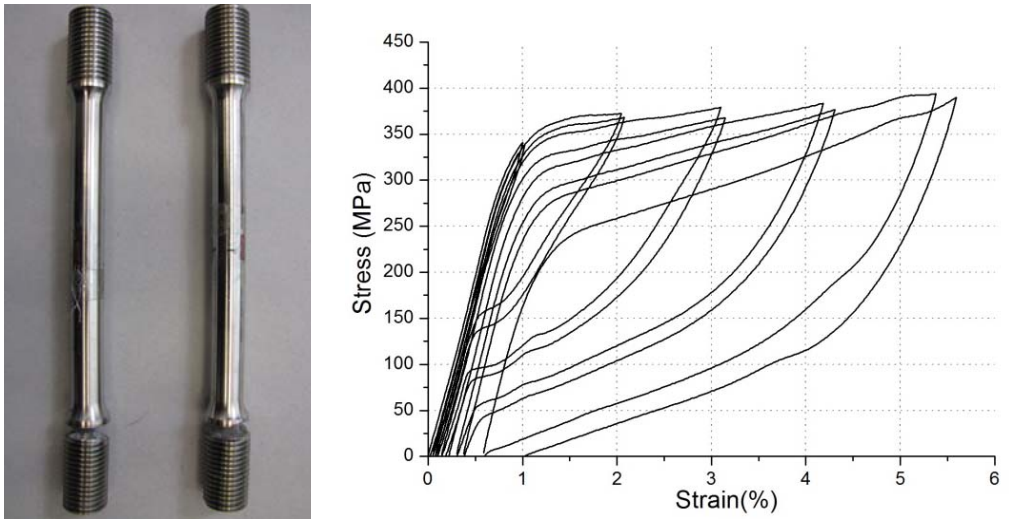

Fig. 2 Dog bone tensile specimen and typical stress-strain response of SMA bolt

Linear variable differential transformers (LVDTs) were employed to measure the displacements and movements of the connection during the loading process, where the layout is shown in Fig. 3. LVDTs 1 and 2 were placed at the two external bolts heads to measure the deformations of the SMA bolts; LVDTs 3, 4 and 5 were used to measure the deformation of the end-plate, where the difference of reading between the top and bottoms LVDTs (i.e., LVDTs 3 and 4) was used to obtain the concentrated rotation of the connection; and LVDT 6 was mounted at the loading position to measure the overall drift of the beam-to-column sub-frame. Although the column was designed to have negligible deformation, two additional LVDTs 7 and 8 were placed at the column face to measure any possible minor rotation (rigid movement) caused by the column. Typical layouts of strain gauges are also illustrated in Fig. 3. For each SMA bolt, two strain gauges were mounted along the bolt shank at the mid-length at the top and bottom sides. The main function of these strain gauges was to monitor the preload condition of the SMA bolts to ensure the preload requirement of approximately 70% of the forward transformation stress. Strain gauges were also mounted on the beam flanges and the end-plate, and these were used to check that the beam and the end-plate have no plastic deformation during the cyclic loading, such that the main inelastic rotation was contributed by the SMA bolts. Two additional strain gauges were mounted at the top and bottom beam stiffeners to monitor any possible plastic deformation of the

stiffeners. The cyclic load was applied using a displacement control, where the loading protocol is according to the SAC project recommendation (SAC 1997). The SAC protocol uses drift angle as the main parameter, and the sequence of loading drifts are: 0.375% (six cycles), 0.50% (six cycles), 0.75% (six cycles), 1% (four cycles), 1.5% (two cycles), 2% (two cycles), 3% (two cycles), and finally 4% (two cycles). The load was applied statically in this study.

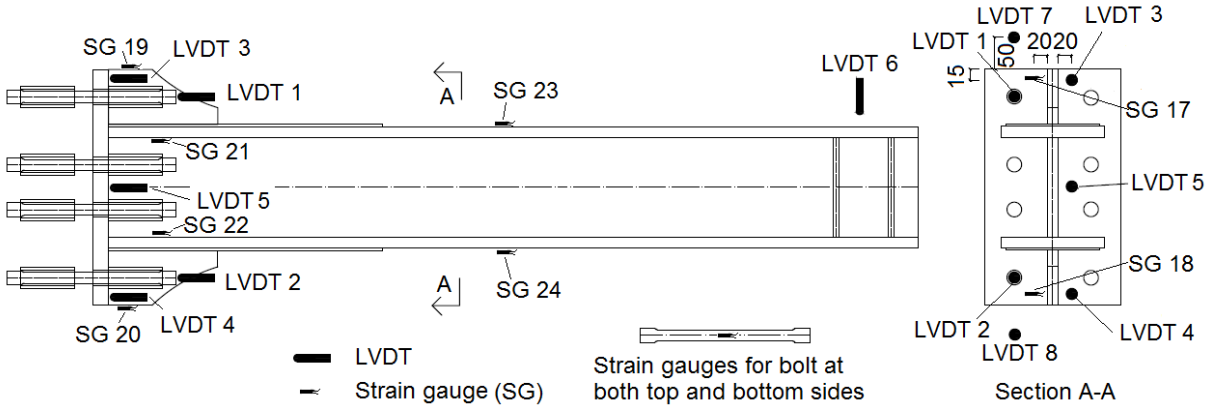

Fig. 3 Instrumentations for test specimens

3. TEST RESULTS AND DISCUSSION

3.1 General

In this section, ‘drift’ is defined as the total rotation of the cantilever beam, i.e., the beam tip deflection (LVDT6) divided by the beam arm length; while ‘concentration rotation’ is the rotation contributed by the connection area, i.e., the difference between the readings of LVDT3 and LVDT4 divided by their distance. Under the adopted cyclic loading protocols, the moment-concentrated rotation (concentrated rotation is simply named as rotation hereafter) responses of the two connections are shown in Fig. 4, where the deformed shape is also shown. In general, the two specimens with two different overall bolt lengths (240 mm and 290 mm) had a similar response. Due to the preload of 70% of the transformation stress, forward transformation of the SMA bolts was already initiated during the initial 0.375% drift cycles (approximately 0.22% rotation), as indicated by the inelastic moment-rotation curves featuring minor energy dissipation. Until the 0.75% drift cycles (approximately 0.5% rotation), similar moment-rotation responses were observed. From the 1.0% drift cycles (approximately 0.7% rotation) onwards, a more recognizable hysteresis with moderate energy dissipation started to show, and the hysteretic curve continued with the increasing of drift until the occurrence of initial bolt fracture. The maximum moment achieved for both connections was 85 kNm. The maximum rotations (ductility supplies) for 240 mm and 290 mm bolt length connections during the cycle prior to the final failure cycle were 0.018 radians and 0.024 radians, respectively, where the maximum strains induced in the SMA bolts

for both connections were approximately 3.2% (deduced from LVDTs). The hysteretic responses of the specimens were quite stable until 1% drift, beyond which a slight softening of the ascending moment-rotation curve was observed.

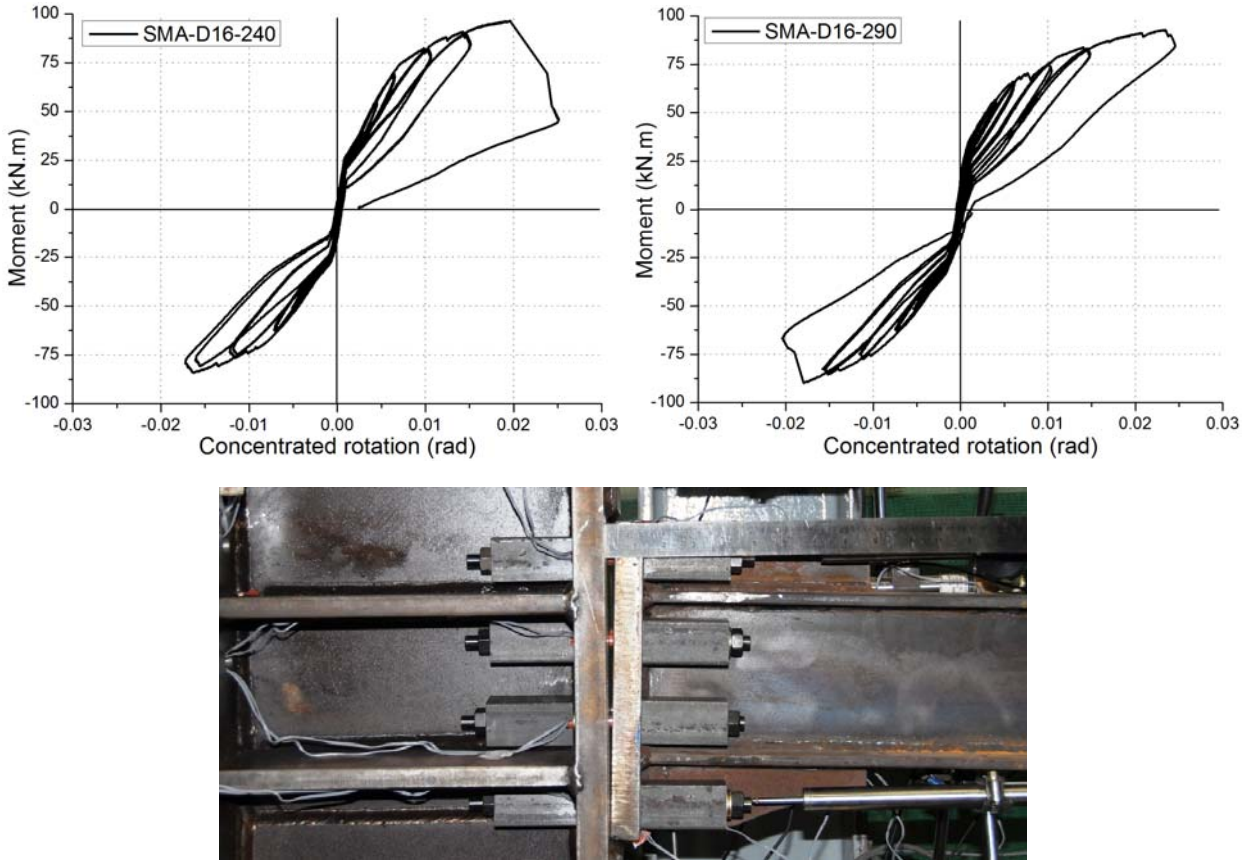

Fig. 4 Moment-rotation response and deformed shape of test connections

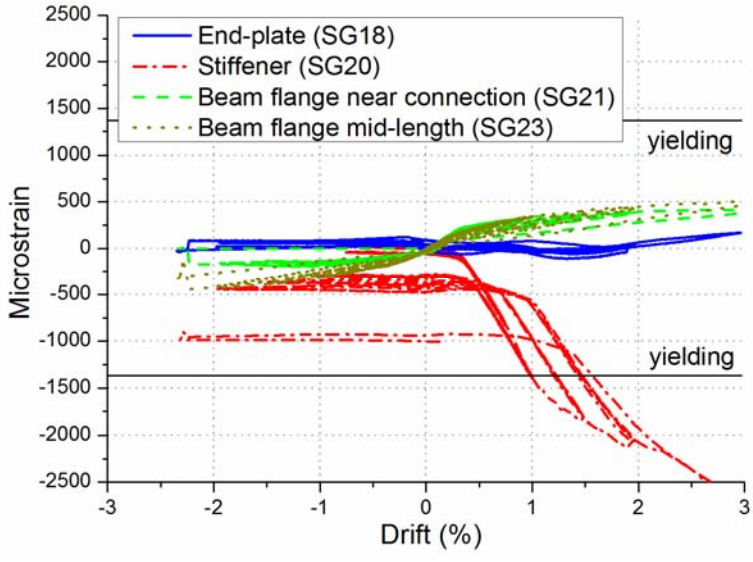

Fig. 5 Typical strain gauge readings

Typical straining gauge readings for the end-plate (SG18), the beam flange stiffeners (SG20), the beam flange near the connection (SG21), and the beam flange at mid-span (SG23) are presented in Fig. 5. The positions of the strain gauge (SG) numbers have been shown Fig. 3. It was observed that the end-plate and the beam remained in the elastic range during the whole loading procedure, and this is in line with the initial design concept that the main inelastic deformation should be concentrated in the SMA bolts. Inelastic deformation was observed in the beam flange stiffeners, and this was due to a relatively large compressive force applied when the connection was rotated, and the stiffeners were located in the 'compression centre.

3.2 Connection rotational stiffness

A connection is usually classified as pinned, semi-rigid, or rigid according to its initial rotational stiffness. The connection rotational stiffness is normally evaluated through comparisons with EI/L, where E, I, and L are the modulus of elasticity, second moment of area, and span of the connected beam, respectively. Eurocode 3 (2005) specifies that a connection is pinned if the initial rotational stiffness is less than 0.5 EI/L, while it is rigid if the initial rotational stiffness is greater than 25EI/L. A connection with the initial rotational stiffness that falls between the two boundaries is classified as semi-rigid. Table 1 presents the initial stiffness and secant stiffness of the connections under the drift levels from 0.375% to 1.0% (mean value of different cycles for each drift). The secant stiffness was obtained by dividing the maximum moment by the maximum rotation for each considered cycle. The ratios of the connection rotational stiffness to EI/L are also given, where the span of the beam was taken as 3.2 m (twice the span of the cantilever beam). It was observed that the ratio of the initial rotational stiffness to EI/L ranged between 10.2 and 11.9, which indicated that the connections were semi-rigid. The secant stiffness was lower with the rotational stiffness over EI/L ratio ranging between 3.7 and 7.0.

Table 1 Connection rotational stiffness

Drift	SMA-D16-240				SMA-D16-290			
	K_{ini}	$K_{ini}/(EI/L)$	K_{sec}	$K_{sec}/(EI/L)$	K_{ini}	$K_{ini}/(EI/L)$	K_{sec}	$K_{sec}/(EI/L)$
0.375%	31742	11.9	16926	6.3	31265	11.7	18818	7.0
0.5%	30884	11.5	14164	5.3	29614	11.1	15657	5.8
0.75%	30145	11.3	11694	4.3	29527	11.0	12217	4.6
1.0%	27387	10.2	9919	3.7	28317	10.6	10047	3.7

Note: the unit for K_{ini} and K_{sec} is kNm/rad.

3.3 Recentring ability

The connections showed very good recentring abilities with limited residual deformations. Fig. 6 shows the residual rotations of the connections at the last cycle of each drift. As shown in the figure, the residual rotation remained within 0.0002 radians

under 2% drift (residual rotation = 1.5% maximum rotation). For specimen SMA-D16-290, the residual rotation under 3% drift was increased to 0.0012; however, this value was still very small compared with the maximum rotation of 0.024 (residual rotation = 5% maximum rotation).

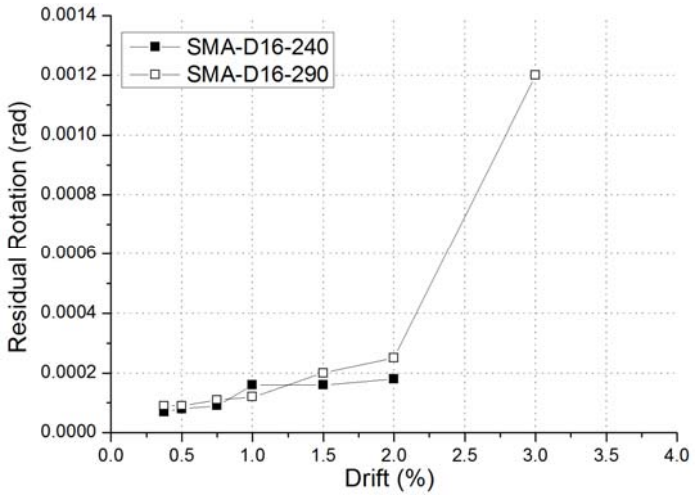

Fig. 6 Residual rotations of test connections

3.4 Energy dissipation

Equivalent viscous damping ξ_{eq} is often adopted to evaluate the energy dissipation capacity of a structural member. The value is given by

$$\xi_{eq} = \frac{W_D}{4\pi W_E} = \frac{W_D}{2\pi K_s \delta_{\max}^2} \tag{1}$$

where the energy loss per cycle W_D, which indicates the energy dissipation capability, is evaluated as the area enveloped by each complete hysteretic cycle; K_s is the secant rotational stiffness in the hysteretic cycle; δ_{max} is the maximum displacement or rotation in the hysteretic cycle, W_E is the energy absorbed in a linear system that has the same maximum rotation and maximum moment. Fig. 7(a) shows the equivalent damping of the connections, where the values at first and second cycles of each drift are separately shown for comparison. The equivalent damping generally increased with the increasing drift. Under initial drifts up to 1.0%, the equivalent damping was between 2% and 4%, which was quite limited. As the more recognizable hysteresis being observed after 1% drift, the equivalent damping started to increase. The maximum value observed in this test was 10.2%. Moreover, it was found that for each drift, the equivalent damping in the second cycle was always less than that in the first cycle. This could be explained by the degradation of ascending moment-rotation response, as typically shown in Fig. 7(b). It should be noted that the properties of SMA can be sensitive to variations of chemical composition, thermal-mechanical heat treatment, history of mechanical deformation,

and specimen geometry being tested, and an optimized control of these aspects could improve the property of NiTi SMA (Huang and Liu 2001, McCormick 2007b, Lagoudas 2008). In particular, it was found in some studies (DesRoches *et al*. 2004, Fugazza 2005) that the degradation effect could be minimised, where the chemical composition and heat treatment was slightly different from those used in the current study. A more detailed discussion on the metallurgy for SMA can be found in these literatures, but this is beyond the scope of this study.

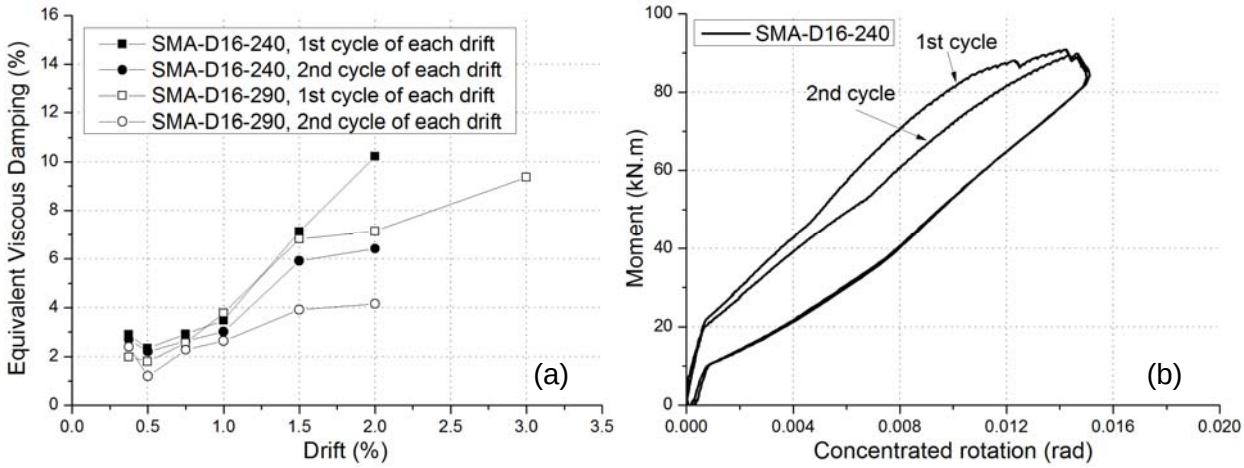

Fig. 7 Equivalent viscous damping and energy dissipation degradation of test connections

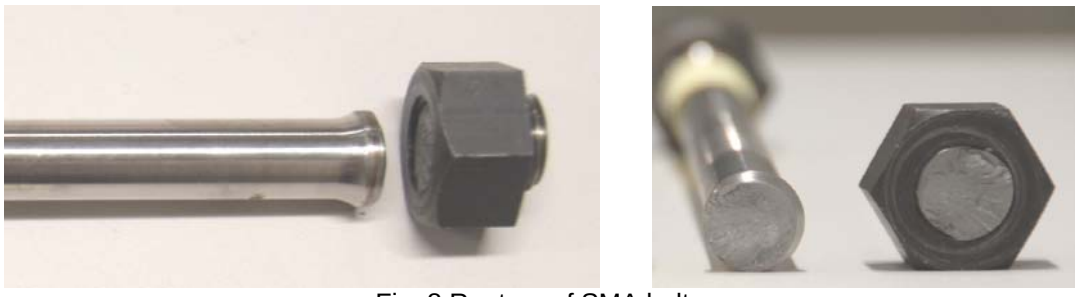
Fig. 8 Rupture of SMA bolts

3.5 Ductility

A good ductility of NiTi SMA wires under an uniaxial loading state was generally observed in other studies (DesRoches *et al*. 2004, Lagoudas 2008); however, the connection ductility observed in this study was less satisfied. The maximum drifts sustained for specimens SMA-D16-240 and SMA-D16-290 were 2% and 3%, respectively, which were governed by SMA bolt rupture over the threaded section. According to Eurocode 8 (2004), the connections under earthquakes should be designed to satisfy that the rotation capacity of the plastic hinge region is not less than 3.5% for structures of Ductility Class High (DCH) and 2.5% for certain structures of Ductility Class Medium (DCM). The AISC (2005) requires that connections should be

designed such that the Special Moment Frame (SMF) and Intermediate Moment Frame (IMF) can accommodate inter-storey drifts of 4% and 2%, respectively. Although different terms are used in the two standards for the definitions of ductility demand, i.e. ‘rotation capacity of the plastic hinge region’ for Eurocode 8 and ‘inter-storey drifts’ for AISC, these terminologies could be considered as equivalent to the ‘drift’ discussed in this study. Based on the codified requirements, the ductility of the test connections can only accommodate small to intermediate design earthquakes.

The major reason for the unsatisfactory ductility for the specimens was because of the ratio of net threaded-to-shank area of the SMA bolts, which was close unity. As shown in Fig. 8, rupture occurred over the threaded area for both specimens. Due to the potential initial imperfection caused by the process of machining, coupling with a minor bending action when the connection deformed, the threaded area could be more vulnerable to rupture. It is believed that the ductility of such connections can be effectively improved by increasing the net section area of the threaded part in future.

4. CONCLUSIONS

A proof-of-concept study on the feasibility of extended end-plate connections equipped with SMA bolts against seismic action is discussed in this paper. Differing from the conventional design concepts for seismic resisting connections, where the main inelastic deformation was forced in the beam for a rigid/full strength connection or in the end-plate for a semi-rigid connection, the basic idea for the new connection was to allow the main deformation concentrated within the SMA bolts, while the remaining part of the connection and the adjacent beam were mainly in the elastic range. One of the potential novel benefits of this design concept was to minimise the post-earthquake repair work which can be difficult and costly. Several promising hysteretic characteristics of the innovative connections were shown, including remarkable recentring / self-healing ability, sufficient rotational stiffness, and moderate energy dissipation. Due to the preloading of the bolts, the shear force was well resisted via friction between the end-plate and the column flange. Ductility of the connections was less satisfied due to the relatively early fracture of the furthest bolt in the threaded area, but it was believed that this issue could be resolved in future through increasing the net threaded area. A small level of degradation of the ascending moment-rotation response was observed as the drift increased beyond 1%, and this was associated with the material characteristics of the SMA bolts. Some studies indicated that the degradation effect could be minimised through a quality control from the perspective of metallurgy, e.g., chemical composition, heat treatment, and forging process. Further collaborations between both communities of material scientists and civil engineers are desirable towards a more confident application of SMA in the civil engineering field.

ACKNOWLEDGEMENT

The work in this paper was supported by a grant from the Research Grants Council of Hong Kong, China (Project No. PolyU 5321/10E). The assistance of Mr. Jiang

Chuanglong and Mr. Tou Ka Man in conducting the tests is acknowledged. The contribution by Dr. Hongwei Ma in designing the test specimens is also acknowledged.

REFERENCES

American Institute of Steel Construction (AISC) (2005), "Seismic provisions for structural steel buildings", Chicago.

DesRoches, R., McCormick, J. and Delemont, M.A. (2004), "Cyclical properties of superelastic shape memory alloys", *J. Struct. Eng.*, **130**, 38-46.

Dolce, M., Cardone, D. and Marnetto, R. (2001), "SMA re-centering devices for seismic isolation of civil structures", *Proceedings of SPIE 238-249*.

Eurocode (2004), "Eurocode 8: Design of structures for earthquake resistance – Part 1: General rules, seismic actions and rules for buildings", Brussels, Belgium.

Eurocode (2005), "Eurocode 3: Design of Steel Structures – Part 1-8: Design of Joints". European Committee for Standardization, Brussels, Belgium.

FEMA 350 (2000), "Recommended seismic design criteria for new steel frame buildings", Federal Emergency Management Agency, Washington, D.C.

Fugazza, D. (2005), "Experimental investigation on the cyclic properties of superelastic NiTi shape-memory alloy wires and bars", Rose School, European school for advanced studies in reduction of seismic risk, Pavia.

Huang, X. and Liu, Y. (2001), "Effect of annealing on the transformation behavior and superelasticity of NiTi shape memory alloy", *Scr. Mater.*, **45**, 153-160.

Jones, S.L., Fry, G.T. and Engelhardt, M.D. (2002), "Experimental evaluation of cyclically loaded reduced beam section moment connections", *J. Struct. Eng.*, **128**, 441-451.

Lagoudas, D.C. (2008), *Shape memory alloys: modeling and engineering applications*, Springer, USA.

Ma, H.W., Wilkinson, T. and Cho, C. (2007), "Feasibility study on a self-centering beam-to-column connection by using the superelastic behavior of SMAs", *Smart. Mater. Struct.*, **16**, 1555-1563.

McCormick, J., DesRoches, R., Fugazza, D. and Auricchio, F. (2007a), "Seismic assessment of concentrically braced steel frames with shape memory alloy braces", *J. Struct. Eng.*, **133**, 862-870.

McCormick, J., Tyber, J., DesRoches, R., Gall, K. and Maier, H.J. (2007b), "Structural engineering with NiTi. II: Mechanical behavior and scaling", *J. Eng. Mech.*, **133**, 1019-1029.

Ocel, J., DesRoches, R., Leon, R.T., Hess, W.G., Krumme, R., Hayes, J.R. and Sweeney, S. (2004), "Steel beam-column connections using shape memory alloys", *J. Struct. Eng.*, **130**, 732-740.

SAC (1997), "Protocol for fabrication, inspection, testing and documentation of beam-column connection test and other experimental specimens", Sacramento, CA: SAC Joint Venture, SAC Rep. SAC/BD-97/02.

Speicher, M.S., DesRoches, R. and Leon, R.T. (2011), "Experimental results of a NiTi shape memory alloy (SMA)-based recentring beam-column connection", *Eng. Struct.*, **33**, 2448-2457.

Wilde, K., Gardoni, P. and Fujino, Y. (2000), “Base isolation system with shape memory alloy device for elevated highway bridges”, *Eng. Struct.*, **22**, 222-229.
Yang, C.S.W., DesRoches, R. and Leon, R.T. (2010), “Design and analysis of braced frames with shape memory alloy and energy-absorbing hybrid devices”, *Eng. Struct.*, **32**, 498-507.